AD-A082 185 SRI INTERNATIONAL MENLO PARK CA F/G 4/1
ON THE SPATIAL RELATIONSHIP OF 1-METER EQUATORIAL IRREGULARITIE--ETC(U)
FEB 79 R T TSUNODA DNA001-79-C-0153

UNCLASSIFIED DNA-4897T NL

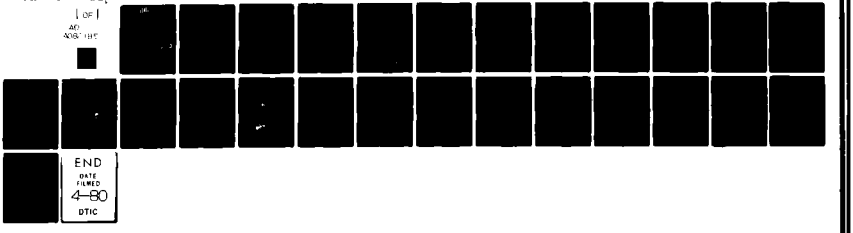

END
DATE FILMED
4-80
DTIC

(12) LEVEL III

DNA 4897T

ON THE SPATIAL RELATIONSHIP OF 1-METER EQUATORIAL IRREGULARITIES AND DEPLETIONS IN TOTAL ELECTRON CONTENTS

Ronald T. Tsunoda
SRI International
333 Ravenswood Avenue
Menlo Park, California 94025

1 February 1979

Topical Report 1 for Period 1 November 1978–31 January 1979

CONTRACT No. DNA 001-79-C-0153

APPROVED FOR PUBLIC RELEASE;
DISTRIBUTION UNLIMITED.

THIS WORK SPONSORED BY THE DEFENSE NUCLEAR AGENCY
UNDER RDT&E RMSS CODE B322079462 I25AAXHX64009 H2590D.

Prepared for
Director
DEFENSE NUCLEAR AGENCY
Washington, D. C. 20305

Destroy this report when it is no longer needed. Do not return to sender.

PLEASE NOTIFY THE DEFENSE NUCLEAR AGENCY, ATTN: STTI, WASHINGTON, D.C. 20305, IF YOUR ADDRESS IS INCORRECT, IF YOU WISH TO BE DELETED FROM THE DISTRIBUTION LIST, OR IF THE ADDRESSEE IS NO LONGER EMPLOYED BY YOUR ORGANIZATION.

UNCLASSIFIED

SECURITY CLASSIFICATION OF THIS PAGE (When Data Entered)

REPORT DOCUMENTATION PAGE		READ INSTRUCTIONS BEFORE COMPLETING FORM
1 REPORT NUMBER DNA 4897T	2. GOVT ACCESSION NO.	3. RECIPIENT'S CATALOG NUMBER
4 TITLE (and Subtitle) ON THE SPATIAL RELATIONSHIP OF 1-METER EQUATORIAL IRREGULARITIES AND DEPLETIONS IN TOTAL ELECTRON CONTENTS		5 TYPE OF REPORT & PERIOD COVERED Topical Report 1 for Period 1 Nov 78—31 Jan 79 6 PERFORMING ORG. REPORT NUMBER SRI Project 8164
7 AUTHOR(s) Roland T. Tsunoda		8 CONTRACT OR GRANT NUMBER(s) DNA 001-79-C-0153
9 PERFORMING ORGANIZATION NAME AND ADDRESS SRI International 333 Ravenswood Avenue Menlo Park, California 94025		10 PROGRAM ELEMENT, PROJECT, TASK AREA & WORK UNIT NUMBERS Subtask I25AAXHX640-09
11 CONTROLLING OFFICE NAME AND ADDRESS Director Defense Nuclear Agency Washington, D.C. 20305		12. REPORT DATE 1 February 1979 13. NUMBER OF PAGES 28
14 MONITORING AGENCY NAME & ADDRESS(if different from Controlling Office)		15. SECURITY CLASS (of this report) UNCLASSIFIED 15a. DECLASSIFICATION DOWNGRADING SCHEDULE

16 DISTRIBUTION STATEMENT (of this Report)

Approved for public release; distribution unlimited.

17 DISTRIBUTION STATEMENT (of the abstract entered in Block 20, if different from Report)

18 SUPPLEMENTARY NOTES

This work sponsored by the Defense Nuclear Agency under RDT&E RMSS Code B322079462 I25AAXHX64009 H2590D.

19 KEY WORDS (Continue on reverse side if necessary and identify by block number)

Equatorial Spread-F
Plasma Bubbles
Radar Backscatter

20 ABSTRACT (Continue on reverse side if necessary and identify by block number)

A radar experiment was conducted at Kwajalein Atoll, Marshall Islands to investigate the spatial relationship of 1-m equatorial spread-F irregularities to total electron content (TEC) depletions. A high-power radar was operated (1) in a backscatter scan mode to spatially map the distribution of 1-m irregularities, and (2) in a dual-frequency, satellite-track mode to obtain the longitudinal TEC variations. Using the radar data, we show that radar backscatter "plumes" found in the disturbed, nighttime equatorial

DD FORM 1 JAN 73 1473 EDITION OF 1 NOV 65 IS OBSOLETE

UNCLASSIFIED

SECURITY CLASSIFICATION OF THIS PAGE (When Data Entered)

20. ABSTRACT (Continued)

ionosphere are longitudinally coincident with TEC depletions. We suggest that the TEC depletions are probably due to the presence of plasma bubbles in the equatorial F layer.

PREFACE

The author would like to thank Dr. D. M. Towle, MIT Lincoln Laboratory, for making the ALTAIR data available and for continued co-operation during the project.

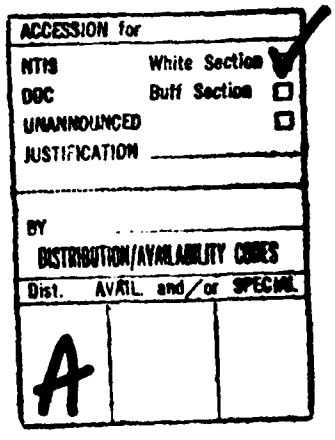

TABLE OF CONTENTS

LIST OF ILLUSTRATIONS

I INTRODUCTION

Recent research on spread-F phenomena in the nighttime equatorial ionosphere has led to the discovery of two unique features, plasma bubbles and radar backscatter plumes. Plasma bubbles are "biteouts" (up to 200 km in diameter) in the F-region ionosphere with electron density depletions up to three orders of magnitude below the ambient level. Radar plumes are regions of strong backscatter produced by field-aligned irregularities (FAI) that extend upward from the bottomside to the topside of the F layer. Plasma bubbles were first observed in ion concentration measurements made by the OGO-6 satellite (Hanson and Sanatani, 1973). Since then, biteouts in plasma density have been detected in-situ by rockets (Kelley et al., 1976; Morse et al., 1977) and by other satellites (McClure et al., 1977; Dyson and Benson, 1978). Radar backscatter plumes have been mapped at 50-MHz by the Jicamarca radar (Farley et al., 1970; Woodman and La Hoz, 1976; Basu et al., 1977), and at 155 MHz by the ALTAIR radar (Tsunoda et al., 1979).

Plasma bubbles have been explained in terms of the Rayleigh-Taylor instability (Dungey, 1956; Hudson and Kennel, 1975). Numerical simulations of the nonlinear evolution of the collisional Rayleigh-Taylor instability by Scannapieco and Ossakow (1976) have shown that plasma depletions develop in the bottomside of the F layer and rise into the topside of the F layer. Furthermore, because of a dominant nonlinearity in two-dimensional models, the bubbles become highly elongated in the vertical direction (Chaturvedi and Ossakow, 1977; Hudson, 1978).

Because radar backscatter plumes are similar in size, shape, and behavior to plasma bubbles, researchers have proposed that the two phenomena are directly associated, if not spatially coincident (Woodman and La Hoz, 1976; McClure et al., 1977). However, thus far, there has been no experimental evidence verifying this hypothesis.

In this report, we present the findings of a radar experiment in which the longitudinal variations of total electron content (TEC) were mapped in the vicinity of radar backscatter plumes. We show that radar backscatter plumes are longitudinally coincident with TEC depletions found in the nighttime equatorial ionosphere. On the basis of evidence presented by other workers, we suggest that the TEC depletions are probably caused by the pre ɔnce of plasma bubbles.

II THE EXPERIMENT

Both radar backscatter plumes and TEC variations were spatially mapped using ALTAIR, a high-power radar, located in the Kwajalein Atoll, Marshall Islands. A description of ALTAIR and its capabilities for equatorial spread-F studies were published by Tsunoda et al. (1979). In contrast to the Jicamarca radar which uses a more or less fixed antenna beam, ALTAIR utilizes a fully-steerable 46-m paraboloid antenna to spatially map equatorial field-aligned irregularities (FAI) in the east-west and near-vertical directions. The angular sector scanned by ALTAIR was 45° in the geomagnetic east-west direction, or approximately 300 km in lateral extent at 400 km altitude.

In addition to mapping equatorial spread-F irregularities at 155.5 MHz, ALTAIR is capable of "skin-tracking" satellites of opportunity at two frequencies (155.5 and 415 MHz) simultaneously. The difference in range (group delay) to the satellite, measured at the two frequencies, provides an absolute measure of the total electron content. The longitudinal distribution of TEC can be determined by tracking east-west orbiting satellites.

On 26 August 1977, ALTAIR was operated in a west-to-east sector-scan mode from 0930 to 1250 UT. (Local time in Kwajalein lags Universal time by 12 hours.) During most of the night a spatial map of backscatter strength was made every six minutes. These scans were interrupted between 1032 and 1040 UT to skin-track the PEOLE (French) satellite. The satellite pass geometry relative to the ALTAIR scans is shown in Figure 1. The location of the point directly beneath the satellite, as a function of time, is shown by the line labeled sub-satellite track. The sub-satellite track is seen to be in a generally west-to-east direction, with an orientation that is slightly north of the east-west plane. The elevation angle to the satellite at the time of closest approach to ALTAIR (1034:54 UT) was 76.7°.

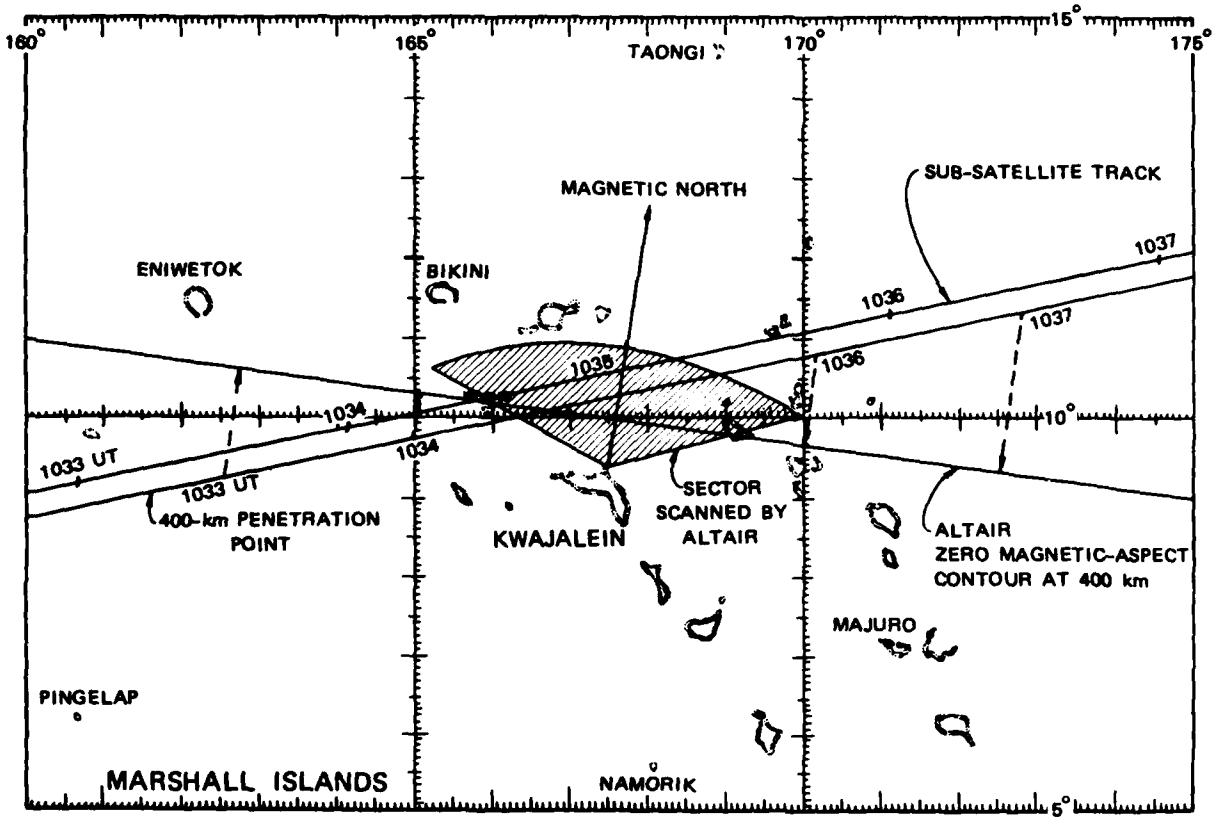

FIGURE 1 SATELLITE PASS GEOMETRY RELATIVE TO THE ALTAIR SCANS

Because the principal ALTAIR radar plumes (described below) to which we compared the TEC variations were centered at an altitude of 400 km, we converted the temporal TEC variations to spatial ones by using that altitude as a reference. The 400-km penetration point (from satellite to ALTAIR) as a function of time is shown in Figure 1 by a line parallel to the sub-satellite track.

Finally, in order to make a direct comparison of spatial TEC variations to backscatter plumes, we projected the TEC spatial variations along the 400-km penetration reference line onto the plane scanned by ALTAIR by assuming that both radar plumes and TEC variations are magnetic field-aligned. For example, the TEC measurements made at 1033 and 1037 UT were projected as shown by the dashed arrows from the 400-km penetration curve onto the geomagnetic east-west line in Figure 1, which is a ground projection of the zero magnetic-aspect contour at 400 km for ALTAIR. With this projection of the TEC variations, the depletions in TEC can be directly compared with the radar plumes mapped by ALTAIR. We note that the projection of the principal TEC variations is no more than 50 km along geomagnetic field lines. Morse et al. (1977) found strong correlation of ionospheric features up to a few hundred kilometers along magnetic flux tubes.

An important feature of this particular experiment geometry is that the PEOLE satellite was at a nominal altitude of 550 km. This means that the TEC variations are produced by electron density variations within the limited altitude range from 550 km down to about 250 km, the altitude of the bottom of the F layer. Therefore, the TEC variations must result directly from the altitude regime containing radar plumes, and are not obscured by electron density variations that might have occurred well above the radar plumes.

III RESULTS

The results are summarized in Figure 2. In the upper panel we have plotted the variation of TEC as a function of magnetic east distance from ALTAIR. (TEC data were available at 3-second intervals, or approximately every 20 km in ground distance.) The times of TEC measurement at given distances from ALTAIR are also shown (above the upper panel). The measured TEC variations are plotted as the irregular boundary of the shaded regions while the smooth boundary is the TEC variations expected from a spherically stratified ionosphere. The smooth curve is included to facilitate identification of TEC depletions and other deviations in the irregular curve. Although the smooth curve was selected arbitrarily, it is consistent with estimates of peak electron density in the quiet F layer (defined as regions with no radar backscatter) computed from ALTAIR incoherent-scatter (IS) measurements. That is, the vertical TEC value is 10^{17} el/m^2 for the smooth curve. If we assume that the applicable layer thickness for the vertical TEC measurement is 300 km, we obtain a mean electron density of 3×10^5 el/cm^3. The ALTAIR IS measurements indicate a value of $3\text{-}4 \times 10^5$ el/cm^3. The shaded regions therefore represent TEC depletions and enhancements presumably associated with plasma bubbles and a generally disturbed equatorial ionosphere.

Major TEC depletions of 45% and 35% were seen directly over ALTAIR around 1035 UT. Other smaller TEC depletions are also seen (in Figure 2) to be distributed across the 1700-km sector scanned with the satellite. In addition to the depletions, there are also TEC enhancements that are as much as 20% above the smooth TEC curve.

The ALTAIR backscatter results are presented in the lower panel of Figure 2. The spatial distribution of field-aligned backscatter was constructed as follows. The 1-m FAI regions were assumed to drift eastward at a nominal speed of 100 m/s (Woodman, 1972). The assumed drift speed was used to space the backscatter maps, taken over ALTAIR at

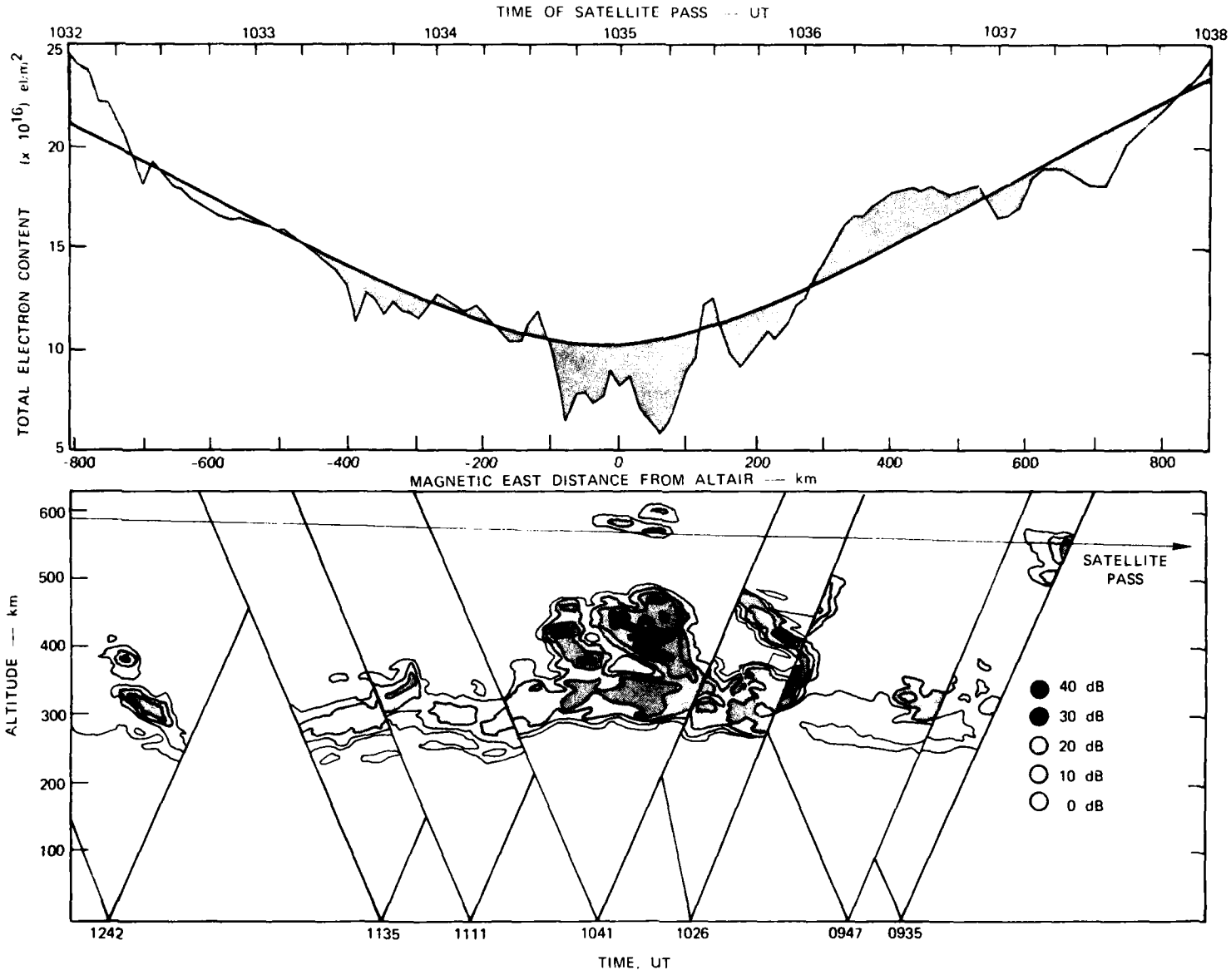

FIGURE 2 COMPARISON OF TOTAL ELECTRON CONTENT VARIATIONS AND ALTAIR BACKSCATTER PLUMES

different times, in the pattern shown in Figure 2. The position of each map, relative to the location of ALTAIR, was based on the time of closest approach of the PEOLE satellite. As can be seen from Figure 2, the TEC measurement over ALTAIR was made at 1035 UT and the corresponding backscatter map was made at 1040:40 UT. The westward displacement of the map is 30 km, based on the assumed 100 m/s eastward-drift speed.

In this analysis, we were primarily interested in comparing the TEC variations measured directly over ALTAIR to the corresponding spatial distribution of radar backscatter plumes. The reason for restricting the analysis to overhead data is that several complications arise when one attempts to make comparisons elsewhere. Comparisons of TEC features located further east and west of ALTAIR require increasing amounts of temporal extrapolation. (We present evidence later in this section that suggests the lifetime of radar backscatter regions is not more than several tens of minutes.) Furthermore, TEC measurements are integrated estimates of the electron density along the line of sight. As a result, low-elevation TEC measurements cannot be simply related to longitudinally-confined but vertically-extended radar plumes.

The spatial relationship between the radar plumes overhead of ALTAIR at 1035 UT and the TEC depletions, shown in Figure 2, is striking. The plumes are seen to be spatially coincident with the TEC biteout that extends from -100 to +100 km from ALTAIR. Even the recovery (at 1035 UT) within the TEC depletion, centered directly over ALTAIR, corresponds to a region of very weak backscatter. The second major TEC depletion (at 1035:45 UT) located at 200 km east of ALTAIR is seen to be also coincident with backscatter that extends upward in altitude (see map taken at 1026 UT). The spatial coincidence of backscatter plumes and TEC biteouts also appears to hold true in the features to the west of ALTAIR, although the relationship is not as convincing as in the overhead comparison. The features that appear to the extreme east and west distances from ALTAIR should not be critically compared because of the required temporal extrapolation and the low elevation angles.

It is also interesting to note that the enhancements in TEC appear to correspond to regions of very weak or of no backscatter. The case in

point is the TEC enhancement located between 300 and 500 km east of ALTAIR. The TEC enhancement at the extreme west distance is also supportive of this relationship.

The conclusion that backscatter plumes are longitudinally coincident with TEC depletions can be strengthened by noting that the patchy backscatter associated with the TEC depletion observed at 1035:45 UT was in fact an intense backscatter plume at earlier times. The time evolution of the backscatter plume is shown in Figure 3. We see that at 0947 UT, there existed an intense, backscatter plume that extended upward to an altitude of 600 km. The next map, taken 39 minutes later at 1026 UT, shows the dissipation of that plume. It seems likely that the backscatter continued to dissipate in the 10 minutes between the map taken at 1026 UT and the satellite pass at 1036 UT. These results suggest that TEC depletions might be more enduring than 1-m FAI.

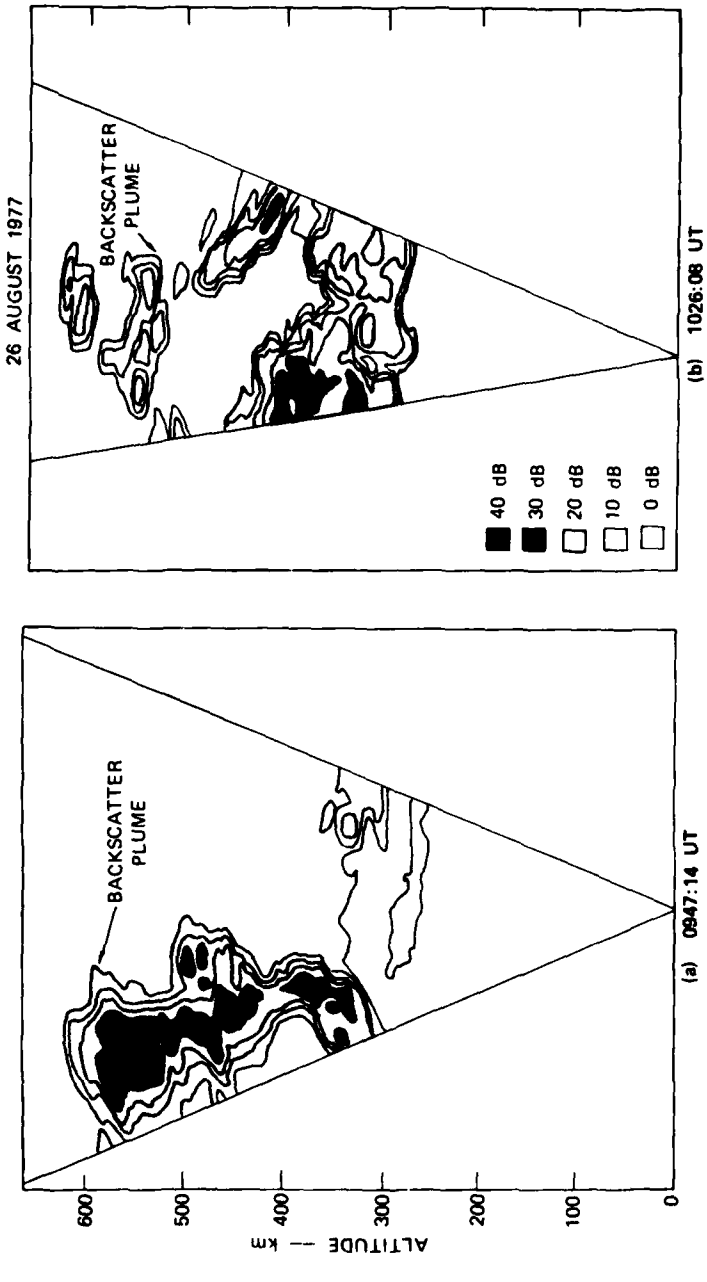

FIGURE 3 TIME SEQUENCE SHOWING THE DECAY OF ALTAIR BACKSCATTER PLUME

IV DISCUSSION AND CONCLUSIONS

The results presented here indicate that backscatter plumes observed with VHF radars are longitudinally coincident with large TEC depletions. Because we know (1) that the altitude of the bottomside F layer was at 250 km, and (2) that the satellite passed at an altitude of 550 km, the TEC depletions must be associated with plasma depletions that occurred within that 300-km altitude interval. Therefore, the TEC depletions must be associated with plasma depletions in the nighttime F layer. On the basis of recent observations of plasma bubbles in the F layer that can be depleted up to three orders of magnitude (Hanson and Sanatani, 1973; McClure et al., 1977), we suggest that the TEC depletions are probably due to plasma bubbles.

Let us consider the implications of the data in terms of a simple plasma-bubble model. The TEC biteout (1034:40 UT) just west of ALTAIR was 35% depleted. That percentage depletion in TEC could also be interpreted as an identical depletion in electron density that extended uniformly from the bottom of the F layer (250 km) to the satellite altitude (550 km). If we assume that the backscatter plume which extends from the bottom of the F layer to an altitude of 450 km defines the volume of the plasma bubble, the electron density within the bubble must be depleted by 53%. Similarly, the TEC depletion of 45% just east of ALTAIR (1035:15 UT) would correspond to a plasma bubble depletion of 69%. In this case, the electron density within the plasma bubble must be $2\text{-}3 \times 10^5$ el/cm^3.

Another possibility is that the plasma bubble is associated with only the upper portion of a backscatter plume and that the remaining backscatter region is associated with the wake left by the rising plasma bubble (Kelley and Ott, 1978). However, it seems unlikely that the volume of the plasma bubble would be much less than, say, a third of the backscatter region. Since the electron density within the plasma bubble would vary inversely as the volume of the bubble, there are clearly

enough electrons within the plasma bubble to produce radar backscatter. On this basis, it is not unreasonable to argue that radar plumes might be spatially coincident with plasma bubbles. In contrast, it is difficult to envision significant backscatter to occur, for example, from within a plasma bubble that is depleted by three orders of magnitude.

The existence of plasma bubbles without significant electron-density fluctuations (McClure et al., 1977) is also consistent with our finding that the lifetime of radar plumes, or equivalently small-scale FAI, is probably shorter than that of a TEC depletion. The rapid development and decay of 1-m FAI are also consistent with results of comparisons between radiowave scintillations and radar plumes (Morse et al., 1977; Basu et al., 1977; 1978). In particular, Basu et al. (1978) have shown that scintillation-producing (large scale) irregularities coexist with backscatter-producing (small scale) irregularities during the generation phase of equatorial FAI in the evening hours. They further showed that the small-scale FAI decay approximately one hour after sunset but that the large-scale FAI persisted.

The presence of 1-m FAI throughout the entire volume of the plasma bubble is not an accepted relationship by the research community because of two reasons: First, all theoretical production mechanisms for small-scale FAI proposed thus far depend on an electron-density gradient, presumably that associated with the walls of the plasma bubble. For example, the Rayleigh-Taylor instability can be considered to be a gravity-driven analog of the gradient-drift instability, the mechanism believed to produce striations in barium ion clouds (Ossakow and Chaturvedi, 1978). In this mechanism, a rising plasma bubble develops gradients on its top side. Radar backscatter should then be associated with the top wall of plasma bubbles. Other researchers have proposed drift waves as a possible source of small-scale FAI (Hudson and Kennel, 1975; Costa and Kelley, 1978; Huba et al., 1978). Drift waves are also dependent on existing electron-density gradients.

Second, there seems to exist a general misconception that all plasma bubbles are depleted by three orders of magnitude. If one assumes that plasma bubbles are all 99.9% depleted, it is of course difficult

to expect significant backscatter from those regions. It should be stressed that 99.9% depletions reported by Hanson and Sanatani (1973) and McClure et al. (1977) represent the most extreme cases. In our data set, the depletion within the plasma bubble (assumed to be the same volume as the radar plume) was no more than 70%. Such a depletion corresponds to an electron density of 2-3 $\times$ 10^5 el/cm^3 within the depleted region. The only way to increase the percentage depletion within the bubble would be to decrease the volume of the bubble. However, if backscatter is presumed to be associated with electron-density gradients, the size of the backscatter region would be smaller than the size of the plasma bubble.

The above discussion leads us to the conclusion that either (1) the radar plume observed with ALTAIR was spatially coincident with a plasma bubble and that the percentage depletion was about 70%, or (2) the percentage depletion was much larger and that part of the radar plume was associated with regions outside the actual plasma bubble. A possible source of 1-m FAI outside the plasma bubble might be the wake region behind the rising plasma bubble (Kelley and Ott, 1978). Vortices produced in the wake will lead to the development of electron-density irregularities if the eddy motion acts on a background electron-density gradient (the bottomside and topside of the F layer).

REFERENCES

Basu, S., S. Basu, J. Aarons, J. P. McClure, and M. D. Cousins, "On the Coexistence of Kilometer- and Meter-Scale Irregularities in the Nighttime Equatorial F Region," J. Geophys. Res., Vol. 83, p. 4219, 1978.

Basu, S., J. Aarons, J. P. McClure, C. La Hoz, A. Bushby, and R. F. Woodman, "Preliminary Comparisons of VHF Radar Maps of F-Region Irregularities with Scintillations in the Equatorial Region," J. Atmos. Terr. Phys., Vol. 39, p. 1251, 1977.

Chaturvedi, P. K. and S. L. Ossakow, "Nonlinear Theory of the Collisional Rayleigh-Taylor Instability in Equatorial Spread F," Geophys. Res. Letts., Vol. 4, p. 558, 1977.

Costa, E. and M. C. Kelley, "Linear Theory for the Collisionless Drift-Wave Instability with Wavelengths Near the Ion Gyroradius," J. Geophys. Res., Vol. 83, p. 4365, 1978.

Dungey, J. W., "Convective Diffusion in the Equatorial F Region," J. Atmos. Terr. Phys., Vol. 9, p. 304, 1956

Dyson, P. L. and R. F. Benson, "Topside Sounder Observations of Equatorial Bubbles," Geophys. Res. Letts., Vol. 5, p. 795, 1978.

Farley, D. T., B. B. Balsley, R. F. Woodman, J. P. McClure, "Equatorial Spread F: Implications of VHF Radar Observations," J. Geophys. Res., Vol. 75, p. 7100, 1970.

Hanson, W. B. and S. Sanatani, "Large Ni Gradients Below the Equatorial F Peak," J. Geophys. Res., Vol. 78, p. 1167, 1973.

Huba, J. D., P. K. Chaturvedi, S. L. Ossakow, and D. M. Towle, "High Frequency Drift Waves with Wavelengths Below the Ion Gyroradius in Equatorial Spread F," Geophys. Res. Letts., Vol. 5, p. 695, 1978.

Hudson, M. K., "Spread F Bubbles: Nonlinear Rayleigh-Taylor Mode in Two Dimensions," J. Geophys. Res., Vol. 83, p. 3189, 1978.

Hudson, M. K. and C. F. Kennel, "Linear Theory of Equatorial Spread F," J. Geophys. Res., Vol. 80, p. 4581, 1975.

Kelley, M. C. and E. Ott, "Two-Dimensional Turbulence in Equatorial Spread F," J. Geophys. Res., Vol. 83, p. 4369, 1978.

Kelley, M. C., G. Haerendel, H. Kappler, A. Valenquela, B. B. Balsley, D. A. Carter, W. L. Ecklund, C. W. Carlson, B. Hausler, R. Torbert, "Evidence for a Rayleigh-Taylor Type Instability and Upwelling of Depleted Density Regions During Equatorial Spread F," Geophys. Res. Letts., Vol. 3, p. 448, 1976.

McClure, J. P., W. B. Hanson, and J. H. Hoffman, "Plasma Bubbles and Irregularities in the Equatorial Ionosphere," J. Geophys. Res., Vol. 82, p. 2650, 1977.

Morse, F. A., B. C. Edgar, H. C. Koons, C. J. Rice, W. J. Heikkila, J. H. Hoffman, B. A. Ti sley, J. D. Winningham, A. B. Christiansen, R. F. Woodman, J. Pomalaza, and N. R. Teixeira, "Equion, An Equatorial Ionospheric Irregularity Experiment," J. Geophys. Res., Vol. 82, p. 578, 1977.

Ossakow, S. L. and P. K. Chaturvedi, "Morphological Studies of Rising Equatorial Spread F Bubbles," J. Geophys. Res., Vol. 83, p. 2085, 1978.

Scannapieco, A. J. and S. L. Ossakow, "Nonlinear Equatorial Spread F," Geophys. Res. Letts., Vol. 3, p. 451, 1976.

Tsunoda, R. T., M. J. Baron, J. Owen, and D. M. Towle, "ALTAIR, An Incoherent-scatter Radar for Equatorial Spread-F Studies," submitted to Radio Science, January 1979.

Woodman, R. F., "East-West Ionospheric Drifts at the Magnetic Equator," Space Res. XII, Vol. 12, p. 969, 1972.

Woodman, R. F. and C. La Hoz, "Radar Observations of F-Region Equatorial Irregularities," J. Geophys. Res., Vol. 81, p. 5447, 1976.

DISTRIBUTION LIST

DEPARTMENT OF DEFENSE

Assistant Secretary of Defense
Comm., Cmd., Cont. & Intell.
ATTN: C3IST&CCS, M. Epstein
ATTN: Dir. of Intelligence Systems, J. Babcock

Assistant to the Secretary of Defense
Atomic Energy
ATTN: Executive Assistant

Command & Control Technical Center
ATTN: C-650, G. Jones
ATTN: C-650
ATTN: C-312, R. Mason
3 cy ATTN: C-650, W. Heidig

Defense Advanced Rsch. Proj. Agency
ATTN: TIO

Defense Communications Agency
ATTN: Code 480, F. Dieter
ATTN: Code R1033, M. Raffensperger
ATTN: Code 205
ATTN: Code 480
ATTN: Code 810, J. Barna
ATTN: Code 101B

Defense Communications Engineer Center
ATTN: Code R123
ATTN: Code R820
ATTN: Code R720, J. Worthington
ATTN: Code R410, J. McLean
ATTN: Code R410, R. Craighill

Defense Intelligence Agency
ATTN: DC-7D, W. Wittig
ATTN: HQ-TR, J. Stewart
ATTN: DT-5
ATTN: DB-4C, E. O'Farrell
ATTN: DB, A. Wise
ATTN: DT-1B

Defense Nuclear Agency
ATTN: DDST
ATTN: STVL
3 cy ATTN: RAAE
4 cy ATTN: TITL

Defense Technical Information Center
12 cy ATTN: DD

Field Command
Defense Nuclear Agency
ATTN: FCPR

Field Command
Defense Nuclear Agency
Livermore Division
ATTN: FCPRL

Interservice Nuclear Weapons School
ATTN: TTV

Joint Chiefs of Staff
ATTN: J-3, WWMCCS Evaluation Office
ATTN: J-37
ATTN: C3S

DEPARTMENT OF DEFENSE (Continued)

Joint Strat Tgt Planning Staff
ATTN: JLTW-2
ATTN: JPST, G. Goetz

National Security Agency
ATTN: W-32, O. Bartlett
ATTN: B-3, F. Leonard
ATTN: R-52, J. Skillman

NATO School (SHAPE)
ATTN: U.S. Documents Officer

Undersecretary of Defense for Rsch. & Engrg.
ATTN: Strategic & Space Systems (OS)

WWMCCS System Engineering Org.
ATTN: R. Crawford

DEPARTMENT OF THE ARMY

Assistant Chief of Staff for Automation & Comm.
Department of the Army
ATTN: DAAC-ZT, P. Kenny

Atmospheric Sciences Laboratory
U.S. Army Electronics R&D Command
ATTN: DELAS-EO, F. Niles

BMD Advanced Technology Center
Department of the Army
ATTN: ATC-T, M. Capps

BMD Systems Command
Department of the Army
2 cy ATTN: BMDSC-HW

Deputy Chief of Staff for Ops. & Plans
Department of the Army
ATTN: DAMO-RQC

Electronics Tech. & Devices Lab.
U.S. Army Electronics R&D Command
ATTN: DELET-ER, H. Bomke

Harry Diamond Laboratories
Department of the Army
ATTN: DELHD-N-RB, R. Williams
ATTN: DELHD-N-P, F. Wimenitz
ATTN: DELHD-I-TL, M. Weiner
ATTN: DELHD-N-P

U.S. Army Comm.-Elec. Engrg. Instal. Agency
ATTN: CCC-EMEO-PED, G. Lane
ATTN: CCC-EMEO, W. Nair
ATTN: CED-CCO, W. Neuendorf

U.S. Army Communications Command
ATTN: CC-OPS-WR, H. Wilson
ATTN: CC-OPS-W

U.S. Army Communications R&D Command
ATTN: DRDCO-COM-RY, W. Kesselman

U.S. Army Foreign Science & Tech. Ctr.
ATTN: DRXST-SD

DEPARTMENT OF THE ARMY (Continued)

U.S. Army Materiel Dev. & Readiness Cmd.
ATTN: DRCLDC, J. Bender

U.S. Army Nuclear & Chemical Agency
ATTN: Library

U.S. Army Satellite Comm. Agency
ATTN: Document Control

U.S. Army TRADOC Systems Analysis Activity
ATTN: ATAA-TDC
ATTN: ATAA-TCC, F. Payan, Jr.
ATTN: ATAA-PL

DEPARTMENT OF THE NAVY

Joint Cruise Missile Project Office
Department of the Navy
ATTN: JCM-G-70

Naval Air Development Center
ATTN: Code 6091, M. Setz

Naval Air Systems Command
ATTN: PMA 271

Naval Electronic Systems Command
ATTN: Code 501A
ATTN: PME 106-4, S. Kearney
ATTN: Code 3101, T. Hughes
ATTN: PME 117-20
ATTN: PME 117-211, B. Kruger
ATTN: PME 117-2013, G. Burnhart
ATTN: PME 106-13, T. Griffin

Naval Intelligence Support Ctr.
ATTN: NISC-50

Naval Ocean Systems Center
ATTN: Code 5322, M. Paulson
ATTN: Code 532, J. Bickel
ATTN: Code 532
3 cy ATTN: Code 5324, W. Moler

Naval Research Laboratory
ATTN: Code 6700, T. Coffey
ATTN: Code 6780, S. Ossakow
ATTN: Code 7500, B. Wald
ATTN: Code 7580
ATTN: Code 7175, J. Johnson
ATTN: Code 7550, J. Davis

Naval Space Surveillance System
ATTN: J. Burton

Naval Surface Weapons Center
ATTN: Code F31

Naval Surface Weapons Center
ATTN: Code F-14, R. Butler

Naval Telecommunications Command
ATTN: Code 341

Office of Naval Research
ATTN: Code 420
ATTN: Code 421

DEPARTMENT OF THE NAVY (Continued)

Office of the Chief of Naval Operations
ATTN: OP 604C
ATTN: OP 941D
ATTN: OP 981N

Strategic Systems Project Office
Department of the Navy
ATTN: NSP-2141
ATTN: NSP-2722, F. Wimberly
ATTN: NSP-43

DEPARTMENT OF THE AIR FORCE

Aerospace Defense Command
Department of the Air Force
ATTN: DC, T. Long

Air Force Avionics Laboratory
ATTN: AAD, W. Hunt
ATTN: AAD, A. Johnson

Air Force Geophysics Laboratory
ATTN: OPR-1, J. Ulwick
ATTN: PHI, J. Buchau
ATTN: LKB, K. Champion
ATTN: OPR, A. Stair
ATTN: PHP, J. Aarons
ATTN: PHP, J. Mullen

Air Force Technical Applications Center
ATTN: TN

Air Force Weapons Laboratory, AFSC
ATTN: SUL
ATTN: DYC

Air Logistics Command
Department of the Air Force
ATTN: OO-ALC/MM, R. Blackburn

Assistant Chief of Staff
Intelligence
Department of the Air Force
ATTN: INED

Assistant Chief of Staff
Studies & Analyses
Department of the Air Force
ATTN: AF/SASC, G. Zank
ATTN: AF/SASC, W. Adams

Ballistic Missile Office
Air Force Systems Command
ATTN: MNNL, S. Kennedy
ATTN: MNNH

Deputy Chief of Staff
Operations Plans and Readiness
Department of the Air Force
ATTN: AFXOXFD
ATTN: AFXOKCD
ATTN: AFXOKS
ATTN: AFXOKT

Electronic Systems Division
Department of the Air Force
ATTN: XRW, J. Deas

DEPARTMENT OF THE AIR FORCE (Continued)

Deputy Chief of Staff
Research, Development, & Acq.
Department of the Air Force
ATTN: AFRDSP
ATTN: AFRDSS
ATTN: AFRDQ
ATTN: AFRDS

Electronic Systems Division
Department of the Air Force
ATTN: DCKC, J. Clark

Electronic Systems Division
Department of the Air Force
ATTN: YSEA
ATTN: YSM, J. Kobelski

Foreign Technology Division
Air Force Systems Command
ATTN: SDEC, A. Oakes
ATTN: NIIS Library
ATTN: TQTD, B. Ballard

Headquarters Space Division
Air Force Systems Command
ATTN: SKA, M. Clavin
ATTN: SKA, C. Rightmyer

Headquarters Space Division
Air Force Systems Command
ATTN: SZJ, W. Mercer
ATTN: SZJ, L. Doan

Rome Air Development Center
Air Force Systems Command
ATTN: TSLD
ATTN: OCS, V. Coyne

Rome Air Development Center
Air Force Systems Command
ATTN: EEP

Strategic Air Command
Department of the Air Force
ATTN: OOKSN
ATTN: DCX
ATTN: DCXT, T. Jorgensen
ATTN: XPFS
ATTN: XPFS, B. Stephan
ATTN: DCXF
ATTN: NRT
ATTN: DCXT
ATTN: ADWATE, B. Bauer

DEPARTMENT OF ENERGY CONTRACTORS

Lawrence Livermore Laboratory
ATTN: Document Control for Technical Information Dept.

Los Alamos Scientific Laboratory
ATTN: Document Control for J. Wolcott
ATTN: Document Control for R. Taschek
ATTN: Document Control for MS 664, J. Zinn
ATTN: Document Control for P. Keaton
ATTN: Document Control for R. Jeffries
ATTN: Document Control for D. Westervelt

DEPARTMENT OF ENERGY CONTRACTORS (Continued)

Sandia Laboratories
ATTN: Document Control for 4241, T. Wright
ATTN: Document Control for Org. 1250, W. Brown
ATTN: Document Control for D. Thornbrough
ATTN: Document Control for D. Dahlgren
ATTN: Document Control for 3141
ATTN: Document Control for Space Project Div.

Sandia Laboratories
Livermore Laboratory
ATTN: Document Control for T. Cook
ATTN: Document Control for B. Murphey

EG&G, Inc.
ATTN: Document Control for D. Wright
ATTN: Document Control for J. Colvin

OTHER GOVERNMENT AGENCIES

Central Intelligence Agency
ATTN: OSI/PSTD

Department of Commerce
National Bureau of Standards
ATTN: Sec. Officer for R. Moore

Department of Commerce
National Oceanic & Atmospheric Admin.
Environmental Research Laboratories
ATTN: R. Grubb

Institute for Telecommunications Sciences
National Telecommunications & Info. Admin.
ATTN: D. Crombie
ATTN: A. Jean
ATTN: L. Berry
ATTN: W. Utlaut

U.S. Coast Guard
Department of Transportation
ATTN: G-DOE-3/TP54, B. Romine

DEPARTMENT OF DEFENSE CONTRACTORS

Aerospace Corp.
ATTN: V. Josephson
ATTN: S. Bower
ATTN: T. Salmi
ATTN: D. Olsen
ATTN: R. Slaughter
ATTN: I. Garfunkel
ATTN: F. Morse
ATTN: N. Stockwell

University of Alaska
ATTN: T. Davis
ATTN: N. Brown
ATTN: Technical Library

Analytical Systems Engineering Corp.
ATTN: Radio Sciences

Analytical Systems Engineering Corp.
ATTN: Security

Barry Research Communications
ATTN: J. McLaughlin

DEPARTMENT OF DEFENSE CONTRACTORS (Continued)

BDM Corp.
ATTN: T. Neighbors
ATTN: L. Jacobs

Berkeley Research Associates, Inc.
ATTN: J. Workman

Boeing Co.
ATTN: J. Kenney
ATTN: D. Murray
ATTN: G. Hall
ATTN: S. Tashird

University of California at San Diego
ATTN: H. Booker

Charles Stark Draper Lab., Inc.
ATTN: D. Cox
ATTN: J. Gilmore

Computer Sciences Corp.
ATTN: J. Spoor
ATTN: H. Blank
ATTN: C. Nail

Comsat Labs
ATTN: G. Hyde
ATTN: R. Taur

Cornell University
ATTN: D. Farley, Jr.

Electrospace Systems, Inc.
ATTN: H. Logston
ATTN: P. Phillips

ESL, Inc.
ATTN: J. Marshall
ATTN: C. Prettie
ATTN: J. Roberts

Ford Aerospace & Communications Corp.
ATTN: J. Mattingley

General Electric Co.
ATTN: M. Bortner

General Electric Co.
ATTN: A. Steinmayer
ATTN: S. Lipson
ATTN: C. Zierdt

General Electric Co.
ATTN: F. Reibert

General Electric Company-TEMPO
ATTN: DASIAC
ATTN: W. Knapp
ATTN: T. Stevens
ATTN: D. Chandler
ATTN: M. Stanton

General Electric Tech. Services Co., Inc.
ATTN: G. Millman

General Research Corp.
ATTN: J. Ise, Jr.
ATTN: J. Garbarino

DEPARTMENT OF DEFENSE CONTRACTORS (Continued)

GTE Sylvania, Inc.
ATTN: M. Cross

HSS, Inc.
ATTN: D. Hansen

IBM Corp.
ATTN: F. Ricci

University of Illinois
ATTN: Security Supervisor for K. Yeh

Institute for Defense Analyses
ATTN: J. Bengston
ATTN: H. Wolfhard
ATTN: E. Bauer
ATTN: J. Aein

International Tel. & Telegraph Corp.
ATTN: G. Wetmore
ATTN: Technical Library

JAYCOR
ATTN: S. Goldman

JAYCOR
ATTN: D. Carlos

Johns Hopkins University
ATTN: T. Potemra
ATTN: P. Komiske
ATTN: Document Librarian
ATTN: T. Evans
ATTN: J. Newland
ATTN: B. Wise

Kaman Sciences Corp.
ATTN: T. Meagher

Linkabit Corp.
ATTN: I. Jacobs

Litton Systems, Inc.
ATTN: R. Grasty

Lockheed Missiles & Space Co., Inc.
ATTN: R. Johnson
ATTN: M. Walt
ATTN: W. Imhof

Lockheed Missiles & Space Co., Inc.
ATTN: D. Churchill
ATTN: Dept. 60-12

University of Lowell Rsch. Foundation
ATTN: K. Bibl

M.I.T. Lincoln Lab.
ATTN: L. Loughlin
ATTN: D. Towle

McDonnell Douglas Corp.
ATTN: W. Olson
ATTN: G. Mroz
ATTN: Technical Library Services
ATTN: N. Harris
ATTN: J. Moule

DEPARTMENT OF DEFENSE CONTRACTORS (Continued)

Mission Research Corp.
ATTN: R. Bogusch
ATTN: R. Hendrick
ATTN: F. Fajen
ATTN: D. Sowle
ATTN: S. Gutsche
ATTN: R. Kilb
ATTN: D. Sappenfield

Mitre Corp.
ATTN: A. Kymmel
ATTN: B. Adams
ATTN: G. Harding
ATTN: C. Callahan

Mitre Corp.
ATTN: J. Wheeler
ATTN: M. Horrocks
ATTN: W. Foster
ATTN: W. Hall

Pacific-Sierra Research Corp.
ATTN: E. Field, Jr.

Pennsylvania State University
ATTN: Ionospheric Research Lab.

Photometrics, Inc.
ATTN: I. Kofsky

Physical Dynamics, Inc.
ATTN: E. Fremouw

R&D Associates
ATTN: M. Gantsweg
ATTN: W. Karzas
ATTN: F. Gilmore
ATTN: R. Turco
ATTN: C. Greifinger
ATTN: C. MacDonald
ATTN: B. Gabbard
ATTN: R. Lelevier
ATTN: H. Ory
ATTN: W. Wright, Jr.

R&D Associates
ATTN: L. Delaney

Rand Corp.
ATTN: E. Bedrozian
ATTN: C. Crain

Riverside Research Institute
ATTN: V. Trapani

Rockwell International Corp.
ATTN: J. Kristof

DEPARTMENT OF DEFENSE CONTRACTORS (Continued)

Santa Fe Corp.
ATTN: E. Ortlieb

Science Applications, Inc.
ATTN: D. Hamlin
ATTN: J. McDougall
ATTN: C. Smith
ATTN: E. Straker
ATTN: D. Sachs
ATTN: L. Linson

Science Applications, Inc.
ATTN: D. Divis

Science Applications, Inc.
ATTN: SZ

SRI International
ATTN: V. Gonzales
ATTN: W. Jaye
ATTN: G. Smith
ATTN: A. Burns
ATTN: G. Price
ATTN: D. Neilson
ATTN: C. Rino
ATTN: D. McDaniels
ATTN: W. Chesnut
ATTN: M. Baron
ATTN: R. Livingston
ATTN: R. Leadabrand
ATTN: R. Hake, Jr.
ATTN: R. Tsunoda

Technology International Corp.
ATTN: W. Boquist

Teledyne Brown Engineering
ATTN: R. Deliberis

Tri-Com, Inc.
ATTN: D. Murray

TRW Defense & Space Sys. Group
ATTN: S. Altschuler
ATTN: R. Plebuch
ATTN: D. Dee

Utah State University
ATTN: K. Baker
ATTN: L. Jensen

Visidyne, Inc.
ATTN: J. Carpenter